Cure Kinetics of An Epoxidized Hemp Oil Based Bioresin System

Nathan W. Manthey, Francisco Cardona, Thiru Aravinthan, Tyson Cooney

Center of Excellence in Engineered Fibre Composites (CEEFC), Faculty of Engineering and Surveying, University of Southern Queensland, Toowoomba, Queensland, Australia 4350

Received 11 January 2011; accepted 13 January 2011
DOI 10.1002/app.34086
Published online 25 April 2011 in Wiley Online Library (wileyonlinelibrary.com).

ABSTRACT: A novel epoxidized hemp oil (EHO) based bioresin was synthesized by epoxidation *in situ* with peroxyacetic acid. In this research the cure kinetics of an EHO based bioresin system cured with triethylenetetramine (TETA) was studied by differential scanning calorimetry using both isothermal and nonisothermal data. The results show that the curing behavior can be modeled with a modified Kamal autocatalytic model that accounts for a shift to a diffusion-controlled reaction postvitrification. The total order of the reaction was found to decrease with an increase in temperature from $\sim$ 5.2 at 110°C to $\sim$ 2.4 at 120°C. Dynamic activation energies were determined from the Kissinger (51.8 kJ/mol) and Ozawa-Flynn-Wall (56.3 kJ/mol) methods. Activation energies determined from the autocatalytic method were 139.5 kJ/mol and −80.5 kJ/mol. The observed negative activation energy is thought to be due to an unidentified competitive reaction that gives rise to the appearance of k_2 decreasing with increasing temperature. The agreement of fit of the model predictions with experimental values was satisfactory for all temperatures. © 2011 Wiley Periodicals, Inc. J Appl Polym Sci 122: 444–451, 2011

Key words: biopolymers; curing of polymers; differential scanning calorimetry; kinetics; renewable resources

INTRODUCTION

The majority of polymer resins used in civil engineering applications are currently derived from nonrenewable, petro-chemical based resources. Due to the performance limitations of thermoplastics in structural applications, there is a sizeable need for research and development into the synthesis and optimization of thermosetting bioresins made from renewable resources. The emergence of fiber reinforced polymer composites in civil engineering, coupled with increasing levels of environmental awareness, has led the Center of Excellence in Engineered Fibre Composites (CEEFC) to research and develop new bioresin systems tailored specifically for civil engineering structural applications. Particular research focus has been placed on the development of epoxidized vegetable oil(s) (EVO) based resins. Epoxidized hemp oil (EHO) has been synthesized at the CEEFC with results comparable to commercial EVO, such as epoxidized linseed oil (ELO) and epoxidized soybean oil (ESO). These EVO resins are sustainable, inexpensive and are also easily incorporated into synthetic epoxy resins as plasticizers or toughening additives. However the production of genuine "green" composites requires that the matrix be manufactured predominately from renewable materials such as EVO.

Numerous complex physical and chemical changes occur during the curing cycle of a thermosetting resin. The physical properties and the processability of thermosetting resins are largely dependent on the reaction rate and degree of cure, which in turn are heavily dependent on the curing conditions, specifically the time and temperature of the cure cycle. It is therefore important to perform cure kinetics studies to establish the optimum processing conditions for thermosetting resins that will provide the required structural performance for specific applications. While extensive cure kinetic studies have been conducted on numerous, different synthetic thermoset systems,[1–14] cure kinetic studies of vegetable oil (VO) based resins, particularly EVO are somewhat limited. Several studies have been conducted by Liang and Chandrashekhara,[15] Liang et al.[16] and Zhu et al.[17] that involve the cure behavior, cure kinetics and rheology analysis of ESO, epoxidized methyl soyate (EMS) and epoxidized allyl soyate (EAS). Badrinarayanan et al.[18] studied the cure kinetics of soybean oil-styrene-DVB thermosetting copolymers. Park et al.[19] performed limited cure characterization of ESO and epoxidized castor oil (ECO) that involved examining the degree of

Correspondence to: N. W. Manthey (nathan.manthey@usq.edu.au).

Contract grant sponsor: Queensland State Government.

TABLE I
Fatty Acid Profile of Raw Industrial Hemp Oil

Fatty acid	%
Palmitic	6.0
Stearic	2.0
Oleic	12.0
Linoleic	57.0
Linolenic	20.7
Other	2.3

cure as a function of temperature. A detailed investigation into the thermal decomposition of epoxidized soybean oil acrylate (ESOA) was performed by Behera and Banthia[20] using related kinetic techniques. Dynamic kinetic analysis was performed on linseed oil (LO) based thermosetting resins by Haman et al.[21] while Tellez et al.[22] conducted thermal analysis and rheological characterization on partially-aminated ELO. Martini et al.[23] conducted a study regarding the curing of ELO methyl esters with different dicarboxylic anhydrides. Souza et al.[24] evaluated the kinetic and thermoanalytic parameters of sunflower oils (SFO) using differential scanning calorimetry (DSC). From the literature it can be observed that the curing characteristics vary for different resin systems and subsequently a variety of kinetic models have been implemented for each different resin system. Due to the gap in the literature regarding cure kinetic studies of EHO resins and also unblended EVO resins, the aim of this research is to determine and model the cure behavior of an EHO based bioresin system using cure kinetics. Dynamic and isothermal cure kinetics using DSC, determination of activation energies and modeling of the cure behavior will be discussed throughout this article.

EXPERIMENTAL

Materials

The cold pressed raw industrial hemp oil used in this study was supplied by Ecofiber, Queensland, Australia. Table I displays the fatty acid profile of the raw industrial hemp oil. Triethylenetetramine (TETA) was used as received from Huntsman.

Synthesis of epoxidized hemp oil

EHO was formed by the epoxidation of cold pressed raw industrial hemp oil (HO) by peroxyacetic acid, formed *in situ* by the reaction of hydrogen peroxide and acetic acid in the presence of an acidic ion exchange resin (Amberlite IR-120 hydrogen form) as the catalyst. A solution of hemp oil (156.25 g, 1 mol), glacial acetic acid (40.04 g, 0.67 mol) and Amberlite IR-120 (23.44 g) were added to a four-necked reaction vessel equipped with a mechanical stirrer and thermometer. The reactor contents were mixed for 5 min prior to dropwise addition of hydrogen peroxide (30% w/v, 113.4 g, 1 mol) for 1 h. The reaction was then performed over a period of 7 h at 110 rpm and 75°C. On completion of the reaction the solution was washed with water three times (cool, hot, cool) to remove the residual peroxyacetic acid and then filtered to remove the catalyst. The resin was dried using a centrifuge and also by aeration. To remove any remaining water, the resin was further dried with anhydrous sodium sulfate (1 : 0.15) in an oven at 70°C for 12 h. The water content after drying using a Sartorius MA-50 moisture analyzer was found to be less than 0.3%. Percentage relative conversion to oxirane and iodine was measured at $\sim$ 88 and 84%, respectively. FT-IR spectroscopy determined $\sim$ 99% consumption of double bonds.

Curing kinetics using DSC

Dynamic and isothermal analysis was performed with a TA instruments DSC Q100 differential scanning calorimeter. An EHO to TETA weight ratio of 100 : 15.4 was used for the analysis. Samples between 15 and 20 mg were enclosed in aluminum DSC sample pans. Dry nitrogen gas at 60 mL/min was used during the experiments to purge the DSC cell. Dynamic scans of EHO samples were performed at four different heating rates 5, 10, 15, and 20°C/min from 15 to 300°C. The cured samples were then cooled to 15°C at a rate of 10°C/min. To complete the heat–cool–heat cycle, the samples were reheated to 300°C to determine the glass transition temperature, T_g and to confirm the nonexistence of any residual curing. Isothermal scans determined from the dynamic DSC data were performed at four different temperatures 110, 115, 117.5, and 120°C. The isothermal scans were deemed to be complete when the thermograms leveled off to a predetermined baseline.

Theoretical analysis

Phenomenological modeling is often used to obtain analytical expressions for the cure kinetics of polymer resins. Depending on the reaction type, an approximated relationship is applied and the parameters are fitted from the experimental data. The most common way of obtaining the data for phenomenological modeling is by DSC. DSC cure kinetic analysis is dependent on the assumption that the heat flow, dH/dt, is proportional to the reaction rate, $d\alpha/dt$. The degree of cure, α, is proportional to the heat generated (exothermic cure reaction) due to

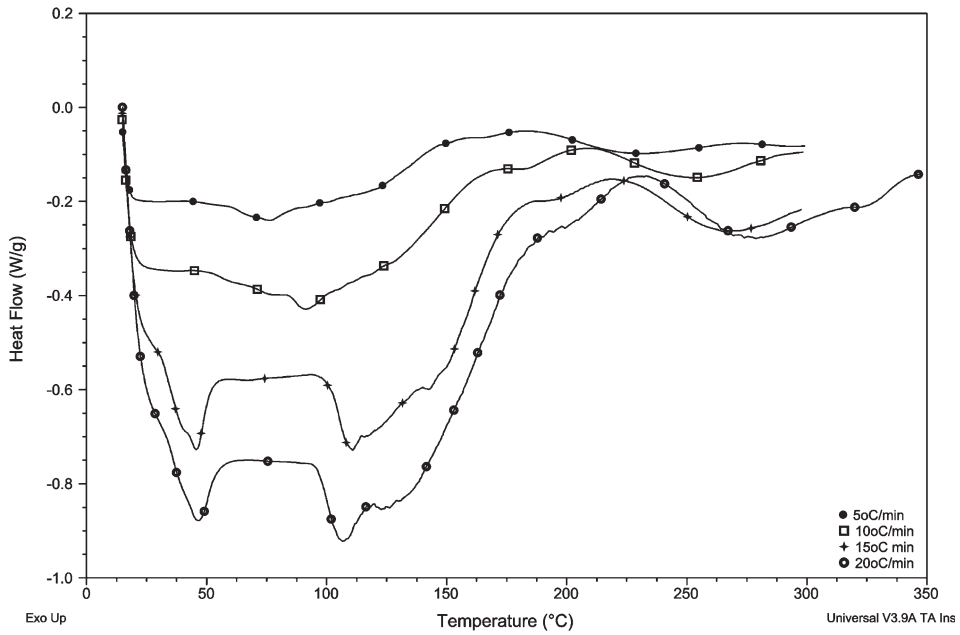

Figure 1 Dynamic DSC curves of EHO based bio-resin at different heating rates.

crosslinking and can be calculated by eq. (1) where, ΔH_t, is the accumulative heat of reaction given from isothermal DSC scans up to a given time, t and ΔH_{total}, is the total reaction heat (averaged from dynamic DSC scans at different heating rates) during the complete reaction. For modeling purposes, it is adequate to consider the total heat of reaction values obtained from dynamic runs to be of the same order as the isothermal heat of reactions plus residual heat of reactions.[12] The reaction rate can be calculated from eq. (2).

$$\alpha = \frac{\Delta H_t}{\Delta H_{\text{total}}} \tag{1}$$

$$\frac{d\alpha}{dt} = \frac{(dH/dt)}{\Delta H_{\text{total}}} \tag{2}$$

Numerous cure kinetic models have been developed to characterize different thermosetting resin systems. However all kinetic models begin with the basic rate equation which is shown in eq. (3). Where, $d\alpha/dt$, is the reaction rate, $k(T)$, is the reaction rate constant that is an Arrhenius function of temperature, $f(\alpha)$, is the function that is dependent on α. $k(T)$ is dependent on temperature and is shown in eq. (4) where, A is the pre-exponential factor, E_a is the activation energy, R is the universal gas constant, and T is the absolute temperature.

$$\frac{d\alpha}{dt} = k(T)f(\alpha) \tag{3}$$

$$k(T)_i = A_i e^{-\frac{E_a}{RT}} \tag{4}$$

Cure kinetics can be analyzed using DSC by two primary methods; dynamic and isothermal. Dynamic kinetic methods use a constant heating rate for a given cycle and are not quantitatively applicable to autocatalytic systems. Isothermal kinetic methods use a constant temperature for a given cycle and are able to be applied to both autocatalytic and nth order systems.

TABLE II
Heats of Reaction and Peak Temperatures at Different Heating Rates

q (°C/min)	ΔH_{total} (J/g)	T_m (°C)
5	87.4	157.2
10	94.6	168.4
15	106.6	182.9
20	120.8	195.3
Avg. ΔH_{total}	102.4	

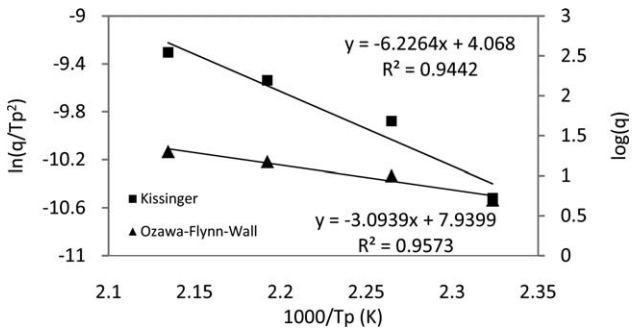

Figure 2 Plots to determine Kissinger and Ozawa-Flynn-Wall activation energies.

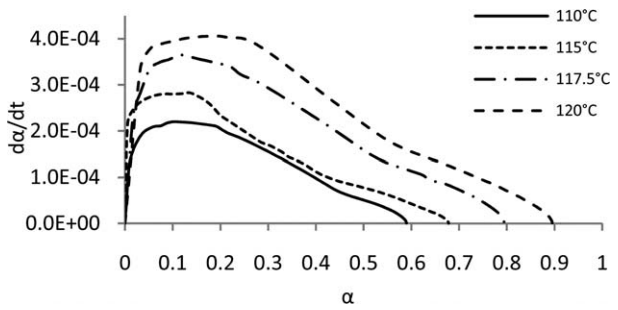

Figure 3 Reaction rate versus degree of cure at different temperatures.

Dynamic analysis

Dynamic kinetic models based on multiple heating rates have been developed by Kissinger[14] and Ozawa-Flynn-Wall.[25,26] Both the Kissinger and Ozawa-Flynn-Wall methods are independent of the reaction order and consequently simplify the complexity of the curing reaction. Therefore it needs to be understood that the determined activation energies are only considered to be approximate values. Kissinger proposes that α at the peak temperature, T_m, is constant and independent of the heating rate, q, for the curing reaction. T_m was determined from the peak of the exotherms at each heating rate using Universal Analysis 2000 version 3.9A software supplied with the DSC Q100. E_a, which is the minimum energy required to initiate a chemical reaction, can be calculated from eq. (5) whereby a plot of ln (q/T_m^2) versus $1/T_m$ will provide E_a over the course of the reaction. Ozawa-Flynn-Wall developed an alternative kinetic model based on Doyle's approximation,[27] eq. (6) where $g(\alpha)$ is a function dependent on α. A plot of log q versus $1/T_m$ will provide E_a over the course of the reaction.

$$\frac{d\left[\ln\left(q/T_m^2\right)\right]}{d(1/T_m)} = -\frac{E_a}{R} \tag{5}$$

$$\log q = \log\left(\frac{AE_a}{g(\alpha)}\right) - 2.315 - \frac{0.4567E_a}{RT_m} \tag{6}$$

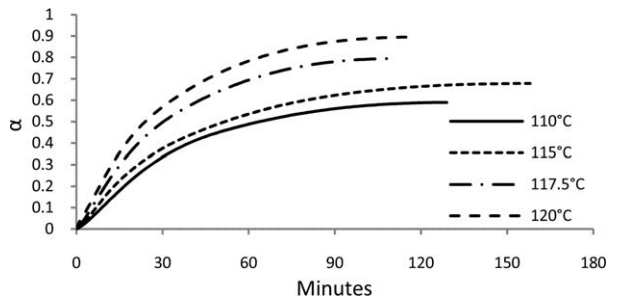

Figure 4 Degree of cure versus time at different temperatures.

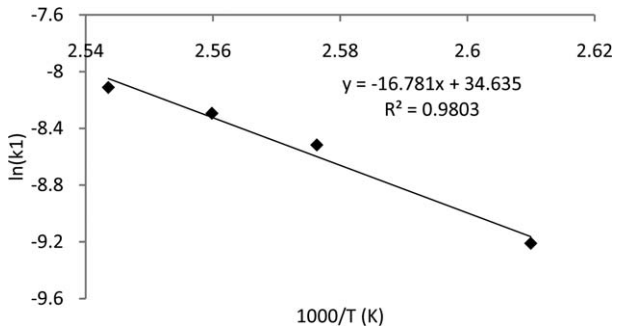

Figure 5 Arrhenius-type plot for reaction constant, k_1.

Isothermal cure kinetics

Generally two different kinetic models are used with regards to thermosetting resins. The simplest kinetic model is the nth order rate equation, eq. (7) below, where k is the reaction rate constant and n is the reaction order.

$$\frac{d\alpha}{dt} = k(1-\alpha)^n \tag{7}$$

Autocatalytic cure reaction models are used to model reactions where one of the reaction products is also a catalyst for further reactions.[28] The cure kinetics of autocatalytic thermosetting resin systems can be expressed by eq. (8), where k is the reaction rate constant and m and n are the reaction orders.[29] This model presents the maximum reaction rate occurring in the intermediate conversion stage ($\alpha \approx 0.2 - 0.4$) as opposed to the model in eq. (7) in which the maximum reaction occurs at the beginning of the reaction process.

$$\frac{d\alpha}{dt} = k\alpha^m(1-\alpha)^n \tag{8}$$

By using multiple reaction rate constants instead of a single reaction rate constant more accurate modeling results can be obtained. Kamal's model,[29]

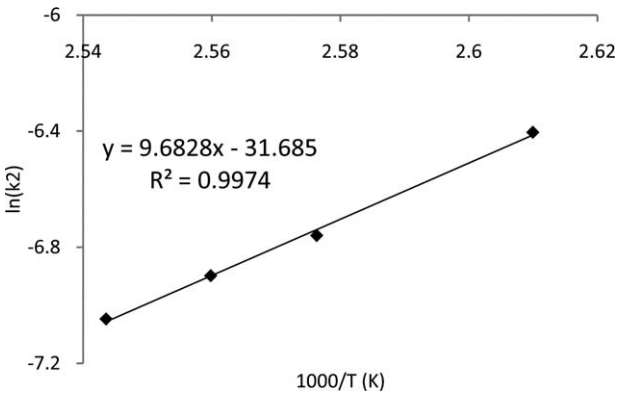

Figure 6 Arrhenius-type plot for reaction constant, k_2.

TABLE III
Kinetic and Diffusional Parameters at Different Temperatures

T (°C)	k_1	k_2	m	n	$m + n$	C	α_c
110.0	0.00010	0.00166	0.8016	4.3779	5.1795	100	0.590
115.0	0.00020	0.00116	0.7484	3.5146	4.2630	140	0.678
117.5	0.00025	0.00101	0.7430	2.3036	3.0466	170	0.794
120.0	0.00030	0.00087	0.7080	1.6425	2.3505	200	0.895

eq. (9), uses two rate constants and has been successfully applied to numerous autocatalytic reactions of a variety of resin systems, where k_1 and k_2 are the reaction rate constants. The nth order uncatalyzed and autocatalytic phenomena are accounted for by k_1 and k_2m, respectively.[30] Further modification of eq. (9) has been proposed, eq. (10). This model incorporates an α_{max} term to prevent the fractional conversion exceeding the degree of cure associated with the vitrification phenomenon that may be observed in isothermal curing.

$$\frac{d\alpha}{dt} = (k_1 + k_2\alpha^m)(1-\alpha)^n \tag{9}$$

$$\frac{d\alpha}{dt} = (k_1 + k_2\alpha^m)(\alpha_{max}-\alpha)^n \tag{10}$$

Postvitrification some resin systems may be controlled by diffusion mechanisms rather than kinetic factors. Equation (9) can be modified to account for diffusion controlled mechanisms, eqs. (11) and (12).[31,32] Where C is a fitted constant, α_c is the critical conversion obtained from eq. (1). When $\alpha < \alpha_c$ the system is characterized as being influenced by chemical control. When $\alpha \approx \alpha_c$, the system is said to be at the onset of diffusion control. Once $\alpha > \alpha_c$, the system is controlled by diffusion mechanisms.

$$\frac{d\alpha}{dt} = (k_1 + k_2\alpha^m)(1-\alpha)^n g(\alpha) \tag{11}$$

$$g(\alpha) = \frac{1}{1 + e^{C(\alpha-\alpha_c)}} \tag{12}$$

RESULTS AND DISCUSSION

Dynamic DSC analysis

The dynamic DSC curves at different heating rates are shown in Figure 1 with the results displayed in Table II. Both peak temperature and total heat of reaction linearly increased with increased heating rates. As listed in Table II, the lowest peak temperature, 157.2°C, occurred at the lowest heating rate, 5°C/min and the highest peak temperature, 195.3°C, occurred at the highest heating rate, 20°C/min.

From the Kissinger [eq. (5)] and Ozawa-Flynn-Wall [eq. (6)] models, the activation energies were determined from the gradients of the plots of ln (q/T_m^2) and log q versus $1/T_m$, respectively, in Figure 2. Due to the observed linearity of both plots, validity of both models is suggested. Activation energies for both Kissinger and Ozawa-Flynn-Wall models proved to be similar, with values of 51.8 and 56.3 kJ/mol, respectively. These results are consistent with the findings of other researchers[1,23,33,34] who also found activation energies from the Ozawa-Flynn-Wall model to be marginally higher than the values determined by the Kissinger model.

Isothermal cure kinetics

Figure 3 shows plots of $d\alpha/dt$ as a function of α for the isothermal temperatures. It was observed that the reaction rate increased as the temperature increased. The lowest and highest reaction rates occurred at the lowest and highest isothermal temperatures respectively. The maximum reaction rates

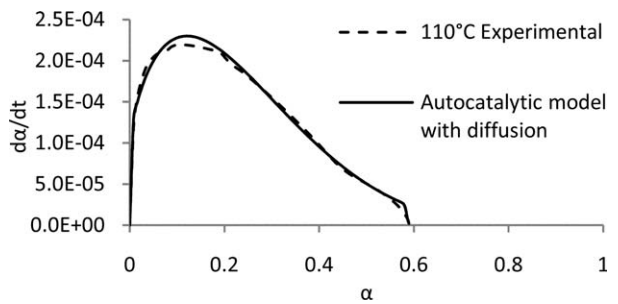

Figure 7 Comparison of experimental data with model predictions for reaction rate versus degree of cure at 110°C.

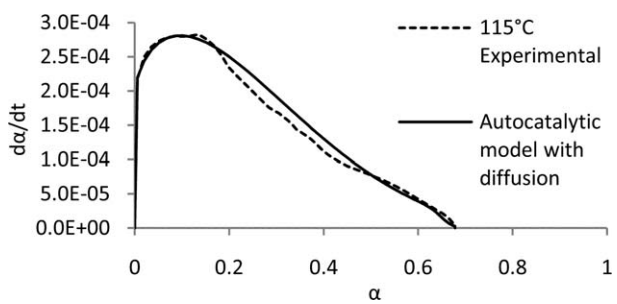

Figure 8 Comparison of experimental data with model predictions for reaction rate versus degree of cure at 115°C.

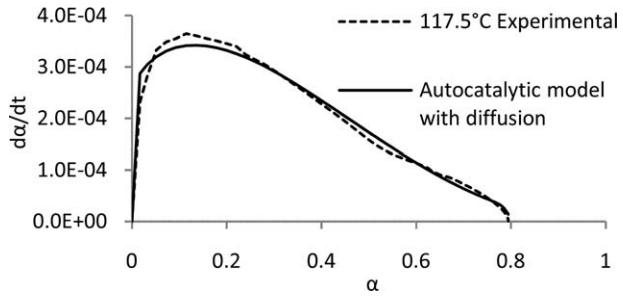

Figure 9 Comparison of experimental data with model predictions for reaction rate versus degree of cure at 117.5°C.

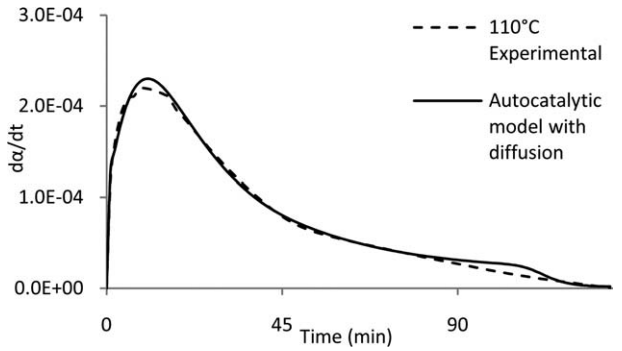

Figure 11 Comparison of experimental data with model predictions for reaction rate versus time at 110°C.

occurred after the beginning of the cure cycle which suggests an autocatalytic reaction as opposed to simple *n*th order kinetics.

Figure 4 displays a series of isothermal reaction curves for the four different isothermal temperatures. The degree of cure was higher at higher temperatures at the same points in time with the maximum degree of cure (0.895) observed at the highest temperature, 120°C. A rapid degree of cure is apparent within the initial stage of the reaction (0–25 min) at all temperatures due to the chemically controlled state of the reaction. Following this stage, the degree of cure begins to slow and level off due to diffusion-controlled mechanisms.

An autocatalytic model, eq. (9), was initially used to model the cure kinetics with unsatisfactory results at higher conversions due to diffusion. A modified form of eq. (9) was used instead [eq. (11)] to account for diffusion in the model. The kinetic parameter, k_1, was determined by extrapolating the isothermal reaction rate curves shown in Figure 3 to $\alpha = 0$. The graphical-analytical method developed by Kenny[13] was used to determine the other kinetic parameters (k_2, m, and n).

The values of the activation energies and the pre-exponential factors were determined by plotting ln $k_{1,2}$ versus $1000/T$, Figures 5 and 6. The activation energies and pre-exponential were determined from the gradients and y-intercepts respectively. The data exhibited a linear form thereby indicating behavior predicted by eq. (4). Computation of the data in Figures 5 and 6 generated values of $E_{a1} = 139.5$kJ/mol, $A_1 = e^{34.64}$, $E_{a2} = -80.5$kJ/mol, and $A_2 = e^{-31.69}$. E_{a2} displays anti-Arrhenius behavior as k_2 was found to decrease with temperature therefore implying a negative activation energy. The nature and cause of this behavior has not been identified. This observed negative activation energy is thought to be due to an unidentified competitive reaction that gives rise to the appearance of k_2 decreasing with increasing temperature.[35] From Table III it can be seen that as the temperature increased the values of k_1 increased and k_2 decreased. The higher values of k_2 compared with values of k_1 suggests that the reaction may be more influenced by autocatalytic mechanisms as opposed to *n*th order unanalyzed mechanisms. Values of m and n were found to decrease when the temperature increased. Subsequently the overall reaction order was found to decrease with an increase in temperature from a maximum value of ~ 5.2 at 110°C to ~ 2.35 at 120°C.

By applying the determined values of $E_{a1,2}$ and $A_{1,2}$ to eq. (4), applying eqs. (13–15) to eq. (11), the following cure kinetic expression, eq. (16), can be

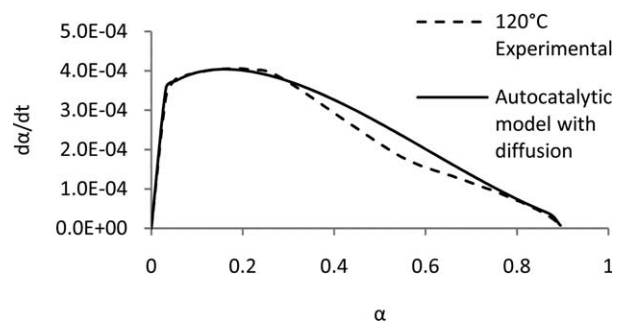

Figure 10 Comparison of experimental data with model predictions for reaction rate versus degree of cure at 120°C.

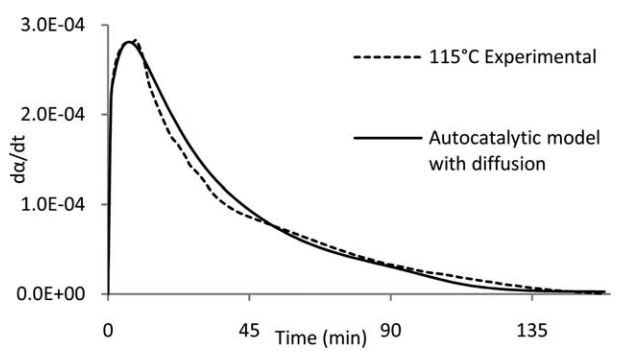

Figure 12 Comparison of experimental data with model predictions for reaction rate versus time at 115°C.

developed for the EHO based bioresin cured with TETA.

$$m \approx m^* = -0.0089(T) + 4.206 \quad (13)$$

$$n \approx n^* = -0.2801(T) + 111.85 \quad (14)$$

$$g(\alpha) \approx g(\alpha)^* = \frac{1}{1 + e^{(9.95(T)-3713)[\alpha-(0.0304(T)-11.08)]}} \quad (15)$$

$$\frac{d\alpha}{dt} = \left(e^{34.64}e^{\left(-\frac{16778.9}{T}\right)} + e^{-31.69}e^{\left(\frac{9680.1}{T}\right)}\alpha^{m^*}\right)(1-\alpha)^{n^*} g(\alpha)^* \quad (16)$$

Figures 7–14 display the results of experimental data and model predictions for reaction rate as a function of degree of cure and time, respectively, for all temperatures. The agreement of fit is satisfactory for all temperatures suggesting the ability of an autocatalytic model with diffusion to predict the curing behavior of the EHO based bioresin cured with TETA.

CONCLUSION

The cure kinetics of an EHO based bioresin system cured with TETA was investigated and characterized by thermal analysis using DSC. Activation energies were calculated using the Kissinger (51.8 kJ/mol), Ozawa-Flynn-Wall (56.3 kJ/mol) and autocatalytic methods (139.5 and −80.5 kJ/mol). The observed negative activation energy is thought to be due to an unidentified competitive reaction that gives rise to the appearance of k_2 decreasing with increasing temperature. Further research work is required to identify the nature of this competitive reaction related to k_2. The total order of the reaction was found to decrease with an increase in temperature from a maximum value of $\sim$ 5.2 to a minimum value of $\sim$ 2.4. An increase in the degree of cure was observed with an increase in temperature with the maximum degree of cure (0.895) observed at 120°C. When the degree of cure progressed through time the reaction rate gradually decreased before finally leveling off to zero due to diffusion-controlled mechanisms. An autocatalytic model, modified to include the diffusion-controlled mechanism postvitrification was used for the kinetic model. The agreement of fit of the model predictions with experimental values was satisfactory for all temperatures enabling the developed kinetic model to be used in further numerical modeling of EHO resins or composites containing EHO resins.

Further work which is in progress involves an investigation into the effects of using different hardeners (fast, medium, slow curing) on the cure kinetics of EHO. This investigation will be reported in our next publication.

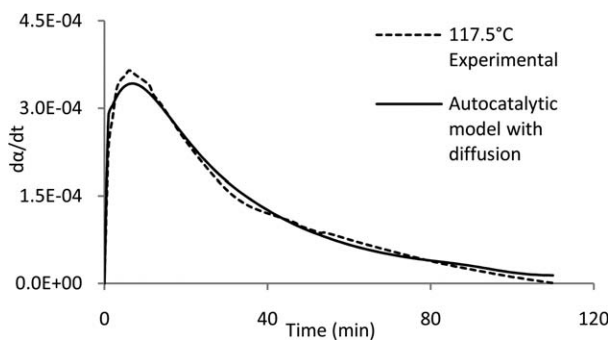

Figure 13 Comparison of experimental data with model predictions for reaction rate versus time at 117.5°C.

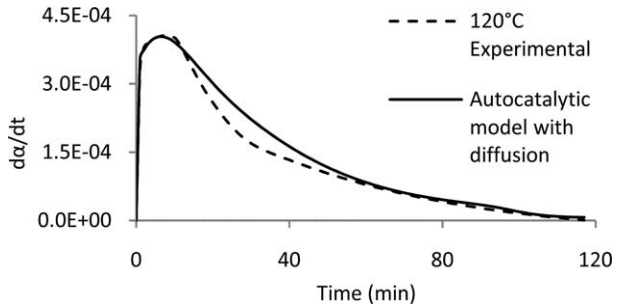

Figure 14 Comparison of experimental data with model predictions for reaction rate versus time at 120°C.

References

1. Chen, W. Y.; Wang, Y. Z.; Chang, F. C. J Appl Polym Sci 2003, 92, 892.
2. Wisanrakkit, G.; Gillham, J. K. J Appl Polym Sci 2003, 41, 2885.
3. Ramos, J. A.; Pagani, N.; Riccardi, C. C.; Borrajo, J.; Goyanes, S. N.; Mondragon, I. POLMAG 2005, 46, 3323.
4. Rosu, D.; Mititelu, A.; Cascaval, C. N. Polym Test 2004, 23, 209.
5. Ghaemy, M.; Rostami, A. A.; Omrani, A. POLYIEI 2005, 55, 279.
6. Mathew, D.; Reghunadhan Nair, C. P.; Krishnan, K.; Ninan, K. N. J Polym Sci Part A: Polym Chem 1999, 37, 1103.
7. Du, S.; Guo, Z. S.; Zhang, B.; Wu, Z. POLYIEI 2003, 53, 1343.
8. Ghaemy, M.; Barghamadi, M.; Behmadi, H. J Appl Polym Sci 2004, 94, 1049.
9. Vyazovkin, S.; Sbirrazzuoli, N. Macromolecules 1996, 29, 1867.
10. Ramirez, C.; Rico, M.; Barral, L.; Diez, J.; Garcia-Garabal, S.; Montero, B. J Therm Anal Calorim 2007, 87, 69.
11. Vyazovkin, S.; Sbirrazzuoli, N. Macromol Chem Phys 1999, 200, 2294.
12. Kenny, J. M.; Trivisano, A. Polym Eng Sci 1991, 31, 1426.
13. Kenny, J. M. J Appl Polym Sci 1994, 51, 761.
14. Kissinger, H. E. Anal Chem 1957, 29, 1702.
15. Liang, G.; Chandrashekhara, K. J Appl Polym Sci 2006, 102, 3168.
16. Liang G.; Garg, A.; Chandrashekhara, K.; Flanigan, V.; Kaplia, S. J. Reinf Plast Compos 2005, 24, 1509.
17. Zhu, J.; Chandrashekhara, K.; Flanigan, V.; Kaplia, S. J Appl Polym Sci 2004, 91, 3513.
18. Badrinarayanan, P.; Yongshang, L.; Larock, R. C.; Kessler, M. R. J Appl Polym Sci 2009, 113, 1042.

19. Park, S. J.; Jin, F. L.; Lee, J. R. Macromol Rapid Commun 2004, 25, 724.
20. Behera, D.; Banthia, A. K. J Appl Polym Sci 2008, 109, 2583.
21. Haman, K.; Badrinarayanan, P.; Kessler, R. M. Polym Int 2009, 58, 738.
22. Tellez, G. L.; Vigueras-Santiago, E.; Hernandez-Lopez, S.; Bilyeu, B. Des Monomers Polym 2008, 11, 435.
23. Martini, D. S.; Braga, B. A.; Samios, D. POLMAG 2009, 50, 2919.
24. Souza de Gouveia, A.; Santos Oliveira, J. C.; Conceicao, M. M.; Silva Dantas, M. C.; Prasad, S. Braz J Chem Eng 2004, 21, 265.
25. Flynn, J. H.; Wall, L. A. J Res Natl Bur Stand Sect A 1966, 42, 487.
26. Ozawa, T. J Therm Anal Calorim 1970, 2, 301.
27. Doyle, C. D. Nature 1965, 3, 290.
28. Pan, H.; Shupe, T. F.; Hse, C. Y. J Appl Polym Sci 2008, 108, 1837.
29. Kamal, M. R. Polym Eng Sci 1974, 14, 231.
30. Karayannidou, G. E.; Achilias, D. S.; Sideridou, I. D. Eur Polym Mater 2006, 42, 3311.
31. Chern, C. S.; Poehlein, G. W. Polym Eng Sci 2004, 7, 788.
32. Cole, K. C. Macromolecules 1991, 24, 3093.
33. Barral, L.; Cano, J.; Lopez, J.; Lopez-Bueno, I.; Nogueira, P.; Abad, J.; Ramirez, C. J Polym Sci Part B: Polym Phys 1999, 38, 351.
34. Islam, M. S.; Pickering, K. L.; Foreman, N. J. J Adhes Sci Technol 2009, 23, 2085.
35. Helfferich, F. G. Kinetics of Multistep Reactions, 2nd ed.; The Netherlands, Elsevier, 2004, Chapter 13, p 429.